Reorganization of Miocene deep water circulation in response to the shoaling of the Central American Seaway

Kerim H. Nisancioglu

Program in Atmospheres, Oceans, and Climate, Department of Earth, Atmospheric, and Planetary Sciences, Massachusetts Institute of Technology, Cambridge, Massachusetts, USA

Maureen E. Raymo

Department of Earth Sciences, Boston University, Boston, Massachusetts, USA

Peter H. Stone

Program in Atmospheres, Oceans, and Climate, Department of Earth, Atmospheric, and Planetary Sciences, Massachusetts Institute of Technology, Cambridge, Massachusetts, USA

Received 5 February 2002; revised 10 August 2002; accepted 26 August 2002; published 11 February 2003.

[1] The response of ocean circulation to the shoaling of the Central American Seaway (CAS) is investigated using the Massachusetts Institute of Technology (MIT) Ocean General Circulation Model (OGCM). In contrast to earlier model studies, it is found that significant amounts of deep water are formed in the North Atlantic prior to the closure of the CAS. However, the circulation pattern is fundamentally different from the modern ocean. In the upper layers of the CAS, there is a relatively strong geostrophic flow from the Pacific to the Atlantic, controlled by the pressure difference across the seaway. However, when the CAS is deeper than the level of North Atlantic Deep Water (NADW) outflow, a significant amount of NADW passes through the CAS to the Pacific Ocean. In the Pacific, the deep water traverses the basin from east to west in a relatively narrow zonal jet, and becomes a southward flowing western boundary current, before it joins with the Antarctic Circumpolar Current (ACC) to the south. This implies that deep sea sediment records from the Miocene Pacific Ocean could have been influenced by relatively young NADW and provides a new framework for the interpretation of geochemical tracer data. Diversification of benthic foraminifer fauna suggests that the CAS shoaled to a depth of about 1000 m toward the end of the middle Miocene. This would have prevented the passage of NADW to the Pacific and established the modern deep water circulation pattern at that time. *INDEX TERMS:* 1620 Global Change: Climate dynamics (3309); 3344 Meteorology and Atmospheric Dynamics: Paleoclimatology; 4255 Oceanography: General: Numerical modeling; 4267 Oceanography: General: Paleoceanography; *KEYWORDS:* paleoceanography, miocene, climate, model, deep water, world ocean

Citation: Nisancioglu, K. H., M. E. Raymo, and P. H. Stone, Reorganization of Miocene deep water circulation in response to the shoaling of the Central American Seaway, *Paleoceanography*, *18*(1), 1006, doi:10.1029/2002PA000767, 2003.

1. Introduction

[2] Some of the most important changes to past ocean circulation and climate have been connected with tectonic events involving the closure or opening of oceanic gateways. The most recent event of this nature was the closure of the Central American Seaway (CAS) between North and South America. The details of the tectonics in the region are complicated and not well constrained. However, the shoaling of the seaway is thought to have been gradual, beginning ~16 Ma at the early to middle Miocene boundary [*Keller and Barron*, 1983; *Duque-Caro*, 1990; *Droxler et al.*, 1998], with final closure at about 3 Ma in the middle Pliocene [*Keigwin*, 1982; *Marshall et al.*, 1982; *Coates et al.*, 1992].

[3] Before the closure of the CAS, water flowed between the Pacific and Atlantic Oceans at a latitude of about 10°N. Experiments with the Hamburg Ocean General Circulation Model (OGCM) suggest that North Atlantic Deep Water (NADW) production was severely reduced, or nonexistent when the CAS was open, due to a flow of relatively fresh Pacific water into the North Atlantic [*Maier-Reimer et al.*, 1990; *Mikolajewicz et al.*, 1993; *Mikolajewicz and Crowley*, 1997]. While some deep sea sediment core data indicate that the production of NADW increased in the early Pliocene as the CAS closed [*Tiedemann and Franz*, 1997; *Haug and Tiedemann*, 1998; *Billups et al.*, 1999], other data suggests that NADW production was significant in the Miocene when the CAS was open [*Keller and Barron*, 1983; *Miller and Fairbanks*, 1985; *Woodruff and Savin*, 1989; *Delaney*, 1990; *Wright et al.*, 1992].

[4] In this study, the structure of the meridional ocean circulation and its sensitivity to flow through the CAS at different depths is reexamined with the Massachusetts Institute of Technology (MIT) OGCM. It is important to note that the opening of the CAS is applied to the control run of the modern ocean, where modern values are used for

0883-8305/03/2002PA000767$12.00

Table 1. Common Parameters Used in Experiments With the MIT Ocean GCM

	Parameters	Value
A_h	Horizontal viscosity	5×10^5 m^2/s
A_z	Vertical viscosity	10^{-3} m^2/s
K_h	Horizontal diffusivity	0
K_z	Vertical diffusivity	5×10^{-5} m^2/s
ΔT_{mom}	Momentum time step	40 min
ΔT_{tracer}	Tracer time step	1 day
S_{max}	GM Maximum slope	0.01
K_I	GM isopycnal diffusivity	10^3 m^2/s
Δz	Thickness of model layers (m)	50, 70, 100, 140, 190, 240, 290, 340, 390, 440, 540, 590, 640, and 690

the boundary conditions. Therefore, the results should be viewed as a sensitivity study of the meridional overturning circulation to an open CAS, with possible connections to ocean circulation before the closure, rather than as a simulation of climate before 3 Ma.

2. Description of the Model and Boundary Conditions

2.1. The MIT OGCM

[5] The MIT OGCM is based on the incompressible, Boussinesq form of the Navier–Stoke's equations. Full details of the equations and solution techniques are described by *Marshall et al.* [1997a, 1997b]. In this study the model is used in the hydrostatic limit, and the horizontal resolution is constant at about 2.8° × 2.8°. The maximum depth is 5200 m and there are 15 vertical levels, with the thickness of the layers gradually increasing from 50 m at the ocean surface to 690 m at the bottom (Table 1). As coarse resolution OGCMs are not capable of resolving mesoscale eddies, and ocean circulation is affected by mixing processes due to these eddies, it is necessary to apply a subgrid-scale parameterization for the advection of tracers (such as temperature and salinity). In this version of the model, the parameterization of *Gent and McWilliams* [1990], together with diffusion of tracers along isopycnals [*Redi*, 1982], is implemented as described by *Griffies* [1998].

2.2. Surface Boundary Conditions

[6] In the experiments, the model ocean is initialized with temperature and salinity fields from the studies of *Levitus and Boyer* [1994] and *Levitus et al.* [1994] at all depths for the month of March, when maximum convection takes place in the North Atlantic [*Marshall and Schott*, 1999]. Subsequently, the surface is forced with observed surface heat and freshwater fluxes, as well as sea surface temperature, i.e., mixed boundary conditions given by

$$K_z \frac{\partial S}{\partial z} = S_R F_W \tag{1}$$

$$K_z \frac{\partial T}{\partial z} = \frac{\Delta z}{\tau_T}(T_{obs} - T) + \frac{Q_{obs}}{\rho_0 C_P} \tag{2}$$

where S_R is a reference salinity taken to be equal to 35 psu, F_W is the net freshwater flux in m/s, due to evaporation, precipitation, and runoff (from rivers and ice discharge), ρ_0 is a reference density, C_P is the specific heat capacity of seawater, and Q_{obs} is the net heat flux into the oceans in W/m^2. The sea surface temperature relaxation time step τ_T is set to 75 days.

[7] Traditionally, when using mixed boundary conditions, the surface freshwater flux (F_W) and the heat flux (Q_{obs}) are diagnosed from a spin-up run using restoring boundary conditions [e.g., *Maier-Reimer et al.*, 1990]. In this study, the diagnosed fluxes are not used because they do not correspond to the observed atmospheric fluxes of heat and freshwater, and numerous model studies have found that GCMs forced with traditional mixed boundary conditions are unrealistically unstable to perturbations in the surface fresh water field [*Marotzke and Willebrand*, 1991; *Mikolajewicz and Maier-Reimer*, 1994; *Tziperman et al.*, 1994].

[8] The annual mean surface freshwater flux is based on precipitation minus evaporation data of *Schmitt et al.* [1989] for the Atlantic and *Baumgartner and Reichel* [1975] for the other oceans, combined with river runoff data of *Perry et al.* [1996], as well as Greenland ice-calving data of *Reeh* [1994] (Figure 1). It should be noted that the Arctic and its influence on the freshwater budget is not represented in the present version of the model. Monthly data for surface heat flux is compiled from an updated version of *Trenberth and Solomon* [1994] [see *Jiang et al.*, 1999]. Monthly wind stress fields are obtained from the data of the European Center for Medium-Range Weather Forecasts (ECMWF) for the years 1980–1986, as computed by *Trenberth et al.* [1989].

2.3. Experiment Implementation

[9] The time steps for the momentum and tracer equations are 40 min and 24 hours, respectively. Both time steps are constant with integration time, and the same values are used for all experiments. Note that the tracer time step is larger than the momentum time step by a factor of 36. This speeds up the relatively slow abyssal processes, and significantly accelerates the convergence of the model to equilibrium [*Bryan*, 1984]. The disadvantage is that it distorts the seasonal cycle [*Danabasoglu et al.*, 1996]. However, the annual mean conditions, which are discussed in this paper, are preserved [*Kamenkovich et al.*, 2002].

[10] The following three model experiments were undertaken to test the sensitivity of ocean circulation to the CAS:

1. CNTR: Control experiment with modern configuration of the continents and bathymetry,
2. CAS2700: Perturbed experiment with the bathymetry of the control experiment modified by introducing a three

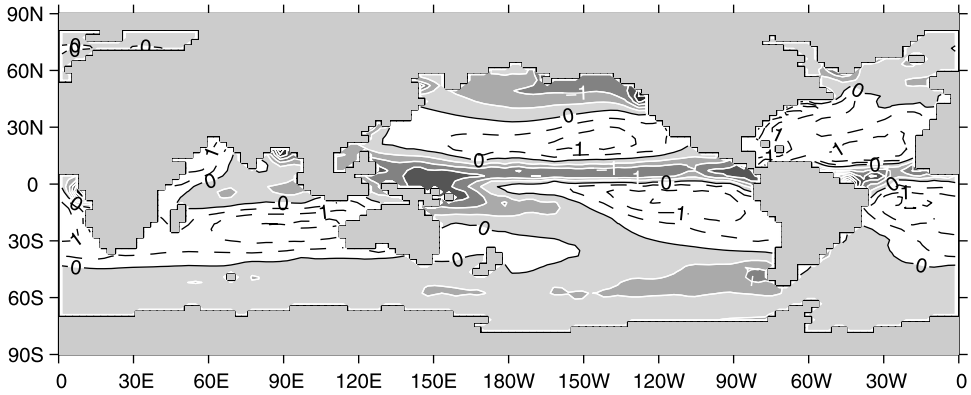

Figure 1. Annual mean surface freshwater flux (F_W) in m/yr equal to evaporation minus precipitation and runoff (from rivers and ice calving).

grid boxes wide and 2700 m deep channel, separating North and South America at latitudes of about 11°–19.5°N,

3. CAS1000: Same as CAS2700, but with a 1000 m deep channel.

The structure of the CAS chosen for experiment CAS2700 is similar to that used by *Maier-Reimer et al.* [1990]. The intermediate sill depth in experiment CAS1000 is chosen, because there is evidence from benthic foraminifera suggesting that the sill could have shoaled to about 1000 m by the end of the middle Miocene (~12.5 Ma) [*Duque-Caro*, 1990]. The same climatological data sets are used for the experiments with an open CAS as for the control experiment.

3. Model Results

3.1. Meridional Overturning Transport

[11] The Eulerian mean meridional overturning stream function, for the Global and Atlantic Oceans of the control experiment (CNTR), shows that the overturning circulation is dominated by the thermohaline cell, originating primarily in the North Atlantic (Figure 2a). This clockwise overturning consists of a warm, relatively saline northward flow in the upper branch, and a cold, southward return flow in the lower branch, recognized as NADW. The maximum strength of the cell is positioned at about 55°N and 1200 m depth in the North Atlantic with an overturning strength of 30 Sv. This is associated with 18 Sv of NADW transport southward across the equator, which agrees well with the modern value of 18 ± 3 Sv, estimated by *Ganachaud* [1999]. From the same figure it can be seen that there is very little Antarctic Bottom Water (AABW) produced in the Atlantic basin of the model. This is thought to be due partly to the lack of a representation of sea ice and the associated brine rejection in the present version of the model.

[12] A comparison of the control (CNTR) with the perturbed experiments (CAS2700 and CAS1000), reveals that the global meridional overturning circulation remains relatively unchanged when the CAS is open (Figures 2b and 2c). The maximum overturning in the Atlantic is reduced to 26 Sv in CAS2700 and CAS1000. Also, the deep southward transport of NADW across the equator in CAS1000 is reduced to 14 Sv. However, in experiment CAS2700 this transport decreases to 6 Sv, which is about one third of the value found in the control experiment. In other words, although the global meridional overturning is relatively strong, the influence of NADW in the South Atlantic appears to be greatly reduced when the CAS is deeper than about 1000 m.

3.2. Surface and Deep Currents

[13] The surface and deep circulation for experiment CNTR (Figures 3a and 4a) correspond reasonably well with the observed currents of the modern ocean. NADW originating in the Labrador and Greenland Seas, flows south as a western boundary current in the Atlantic, before it joins the Antarctic Circumpolar Current (ACC) and eventually upwells in the Pacific and Indian Oceans. A deep western boundary current is also observed in the southern Pacific, where a combination of AABW and NADW flows north from the ACC region.

[14] In experiment CAS2700, the surface circulation (Figures 3b and 3c) does not change much from that of the control experiment, except for a weakening of the western boundary current in the South Atlantic. However, a significant amount of water is shown flowing from the Pacific to the Atlantic. This flow increases in strength below the surface to a maximum at a depth of about 500 m (Figure 5).

[15] At depths below about 1000 m, the flow reverses, and a strong flow from the Atlantic through the CAS to the Pacific is observed. The result is a reduction in the amount of deep water crossing the equator from the North Atlantic to the South Atlantic compared to experiment CNTR, as was observed in the figures of the meridional overturning stream function (Figure 2b). In the same model run, it can be seen that the deep western boundary current in the southern Pacific reverses direction, and flows south toward the ACC region (Figures 4b and 4c). The reversal of the deep western boundary current is observed down to depths of about 3500 m, below which the circulation remains relatively unchanged (not shown).

[16] The deep flow from the Atlantic to the Pacific is caused by the disappearance of the E-W pressure gradient when the western boundary of the Atlantic basin is removed and replaced by the seaway. This allows the deep western boundary current in the Atlantic (which today consists

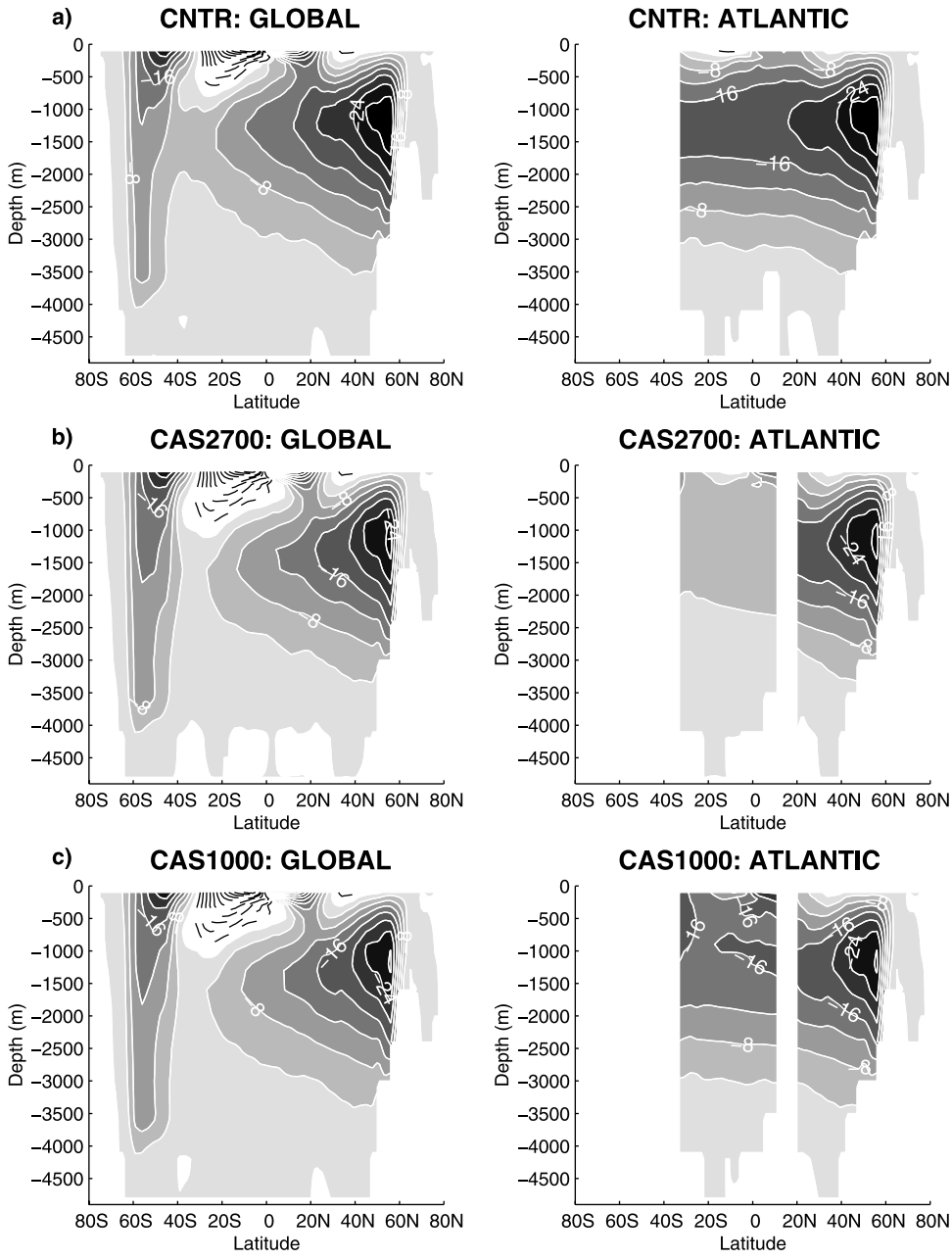

Figure 2. Eulerian mean Meridional Overturning Stream (MOS) function in units of Sv (Sv = 10^6 m^3/s) for the Global and Atlantic oceans. The MOS is calculated from a 10-year mean of meridional velocity after 2000 years of model integration. Negative values (solid contours) imply clockwise overturning, and positive values (stippled contours) imply counterclockwise overturning. The contour interval is 4 Sv. (a) CNTR, (b) CAS2700, and (c) CAS1000.

mostly of NADW) to pass through the CAS to the Pacific, and reduces the southward flow to the South Atlantic. The total eastward and westward transports through the CAS with a sill depth of 2700 m are about 17 and 10 Sv, respectively (Figure 5).

[17] In experiment CAS1000, deep westward transport of NADW through the CAS is prevented by the shallow sill. This sill creates a boundary between the Atlantic and Pacific at depths below 1000 m, which supports the flow of the deep western boundary current to the South Atlantic. Therefore, the transport in the CAS is mainly eastward, with a strength of about 16 Sv (Figure 5).

3.3. Poleward Heat Transport (PHT)

[18] According to *Ganachaud and Wunsch* [2000], the estimated maximum modern PHT by the global ocean is 1.8 ± 0.3 and −0.8 ± 0.6 PW for the Northern and Southern Hemispheres, respectively. These are relatively close to the values found for experiment CNTR, where the maximum PHTs are 1.7 and −1.4 PW (Figure 6a). In this experiment,

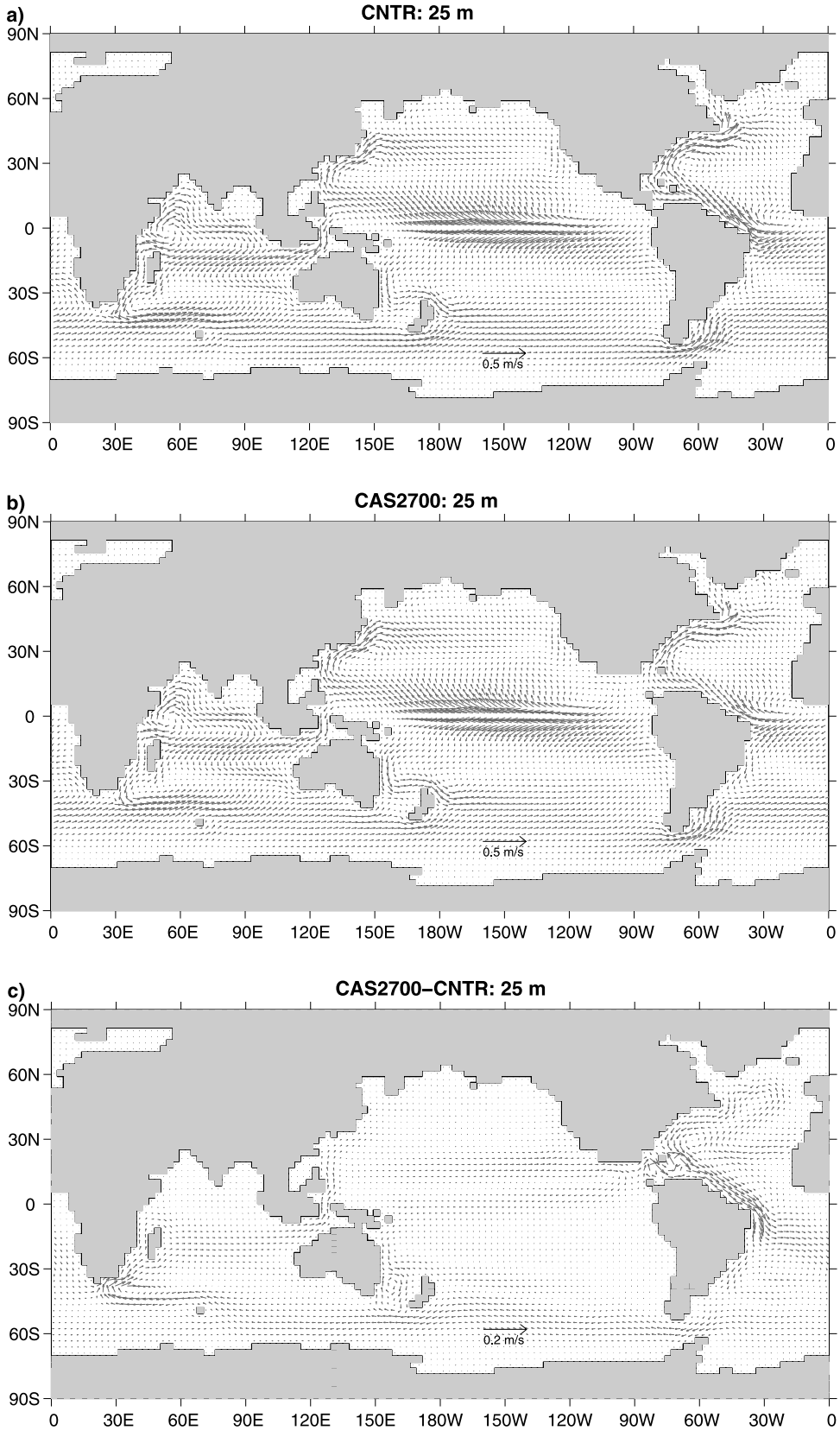

Figure 3. Ocean currents in m/s after 2000 years of model integration at a depth of 25 m for experiments (a) CNTR, (b) CAS2700, and (c) CAS2700 minus CNTR.

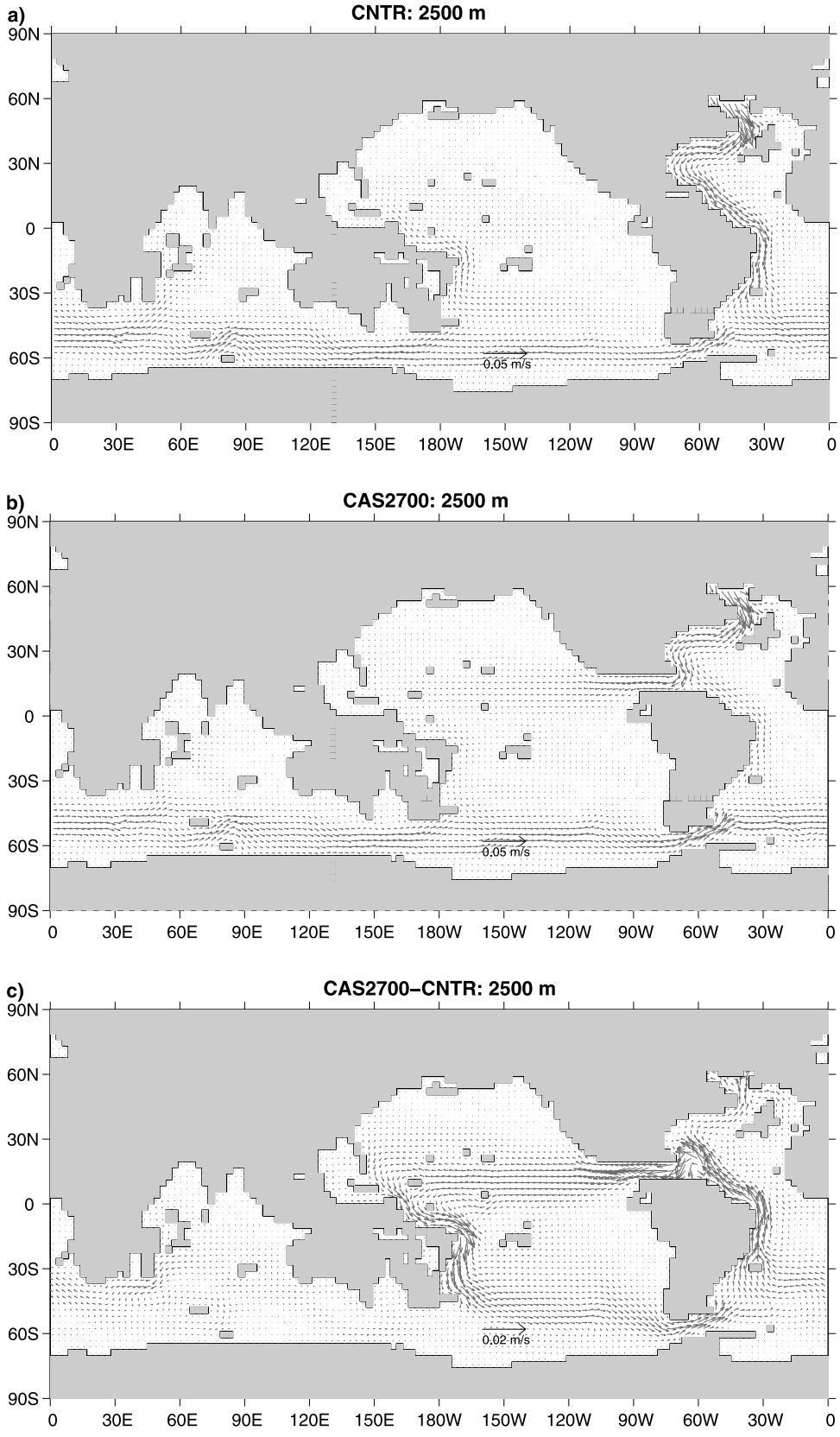

Figure 4. Ocean currents in m/s after 2000 years of model integration at a depth of 2500 m for experiments (a) CNTR, (b) CAS2700, and (c) CAS2700 minus CNTR.

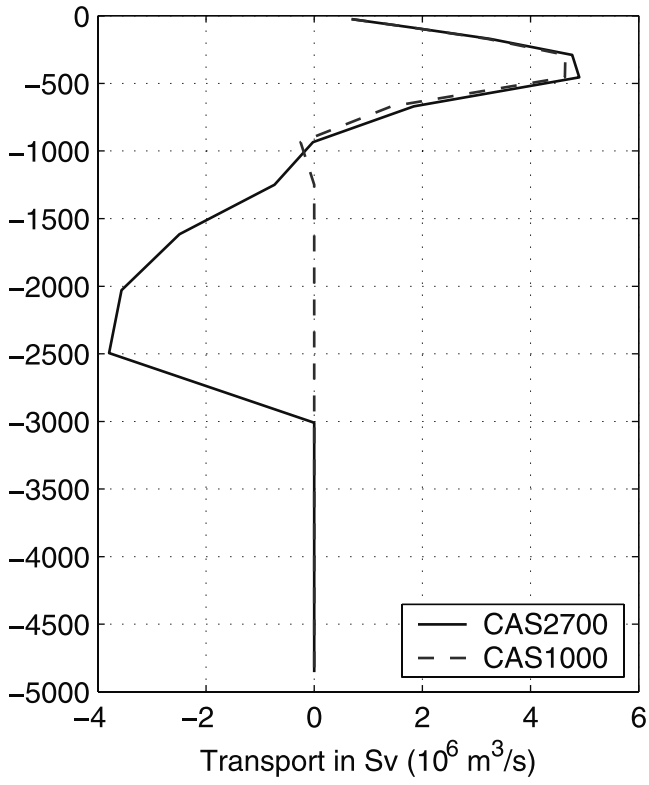

Figure 5. Transport through the CAS in Sv as a function of depth for experiments CAS2700 (solid blue line) and CAS1000 (dashed green line), with sill depths of 2700 and 1000 m, respectively. Positive and negative values imply eastward and westward transport, respectively.

transport by the Atlantic is northward at all latitudes, and dominates the PHT in the Northern Hemisphere, with a smaller northward contribution by the Indo-Pacific. In the Southern Hemisphere, the Indo-Pacific dominates with a strong southward transport.

[19] In experiments CAS2700 and CAS1000, the global PHT in the Northern Hemisphere is reduced by 14% and the global PHT in the Southern Hemisphere is enhanced by 13%, compared to the control experiment. The decrease in the Northern Hemisphere is due to a smaller Atlantic heat transport, whereas the contribution by the Indo-Pacific remains relatively unchanged.

[20] The observed increase in the heat transport in the Southern Hemisphere is linked to the reduced export of NADW south of the equator. In experiment CNTR, 18 Sv of NADW is exported southward across the equator. This has to be balanced by an import of surface waters from the South Atlantic. However, when the NADW export is reduced, as in CAS2700 (6 Sv) and CAS1000 (14 Sv), the import of South Atlantic surface water is reduced as well. The result is a warming of South Atlantic surface waters, and an increase in southward heat transport.

4. Discussion

[21] The model experiments suggest that the shoaling of the CAS had a significant impact on the circulation of the world's oceans. The most notable result is the strong flow through the CAS. This flow is found to vary in strength and direction with depth, and has a significant impact on the global overturning circulation; in particular the deep circulation of the Pacific Ocean.

[22] The experiments show that when the CAS is open, deep water forms in the high latitudes of the North Atlantic (NADW) and passes through the CAS to the Pacific. Once in the Pacific, the deep water flows westward in a relatively narrow zonal jet, and approaches the western boundary of the basin. At the western boundary, the water becomes a southward flowing boundary current, joining with the ACC to the south (see Figure 4b). In the Atlantic, part of the NADW produced flows past the CAS as a western boundary current even when it is open, however, the strength of the current is greatly reduced compared to the control experiment.

[23] These model results are in agreement with the dynamical framework of *Stommel and Arons* [1960a, 1960b] for the abyssal circulation. According to this theory, deep water produced at its source in the modern North Atlantic flows south to the Southern Ocean, where it combines with deep water produced in the Weddell Sea, and increases the transport of the ACC (Figure 7a). This in turn, feeds the northward flowing deep western boundary currents in the Indian and Pacific Oceans, and eventually upwells in the interior of the basins. The opening of the CAS (Figure 7b) is equivalent to introducing a source of deep water at the eastern boundary of the North Pacific, which connects to the western boundary of the basin through a zonal jet. This additional source of deep water in the Pacific results in a reversal of the deep western boundary current, which flows south and joins the ACC.

[24] It is further conceivable that part of the NADW could have continued from the Pacific through the Indonesian Passage and into the Indian Ocean, if the passage was sufficiently deep. However, an investigation of this idea requires further research as the depth of the Indonesian passage and its development through time is uncertain.

4.1. Comparisons With Earlier Model Studies

[25] The results from the experiments presented here differ from earlier model studies with the Hamburg OGCM [*Maier-Reimer et al.*, 1990]. According to the experiments with the Hamburg model, a CAS with a sill depth of about 2700 m, results in a flow of 10 Sv from the Pacific to the North Atlantic. This dilutes the surface salinity in the North Atlantic by >1.0 psu, with the largest changes seen in the subpolar North Atlantic (2.0–3.0 psu fresher). This decrease in salinity prevents the formation of NADW. Thus, no deep flow from the Atlantic to the Pacific is observed in these experiments, due to the negligible production of deep water in the North Atlantic, and the concomitant reduction in the strength of the deep western boundary current.

[26] In the experiments presented here, the North Atlantic is freshened by about 0.5 psu at latitudes above ~30°N, due to the eastward flow in the upper layers of the CAS. This

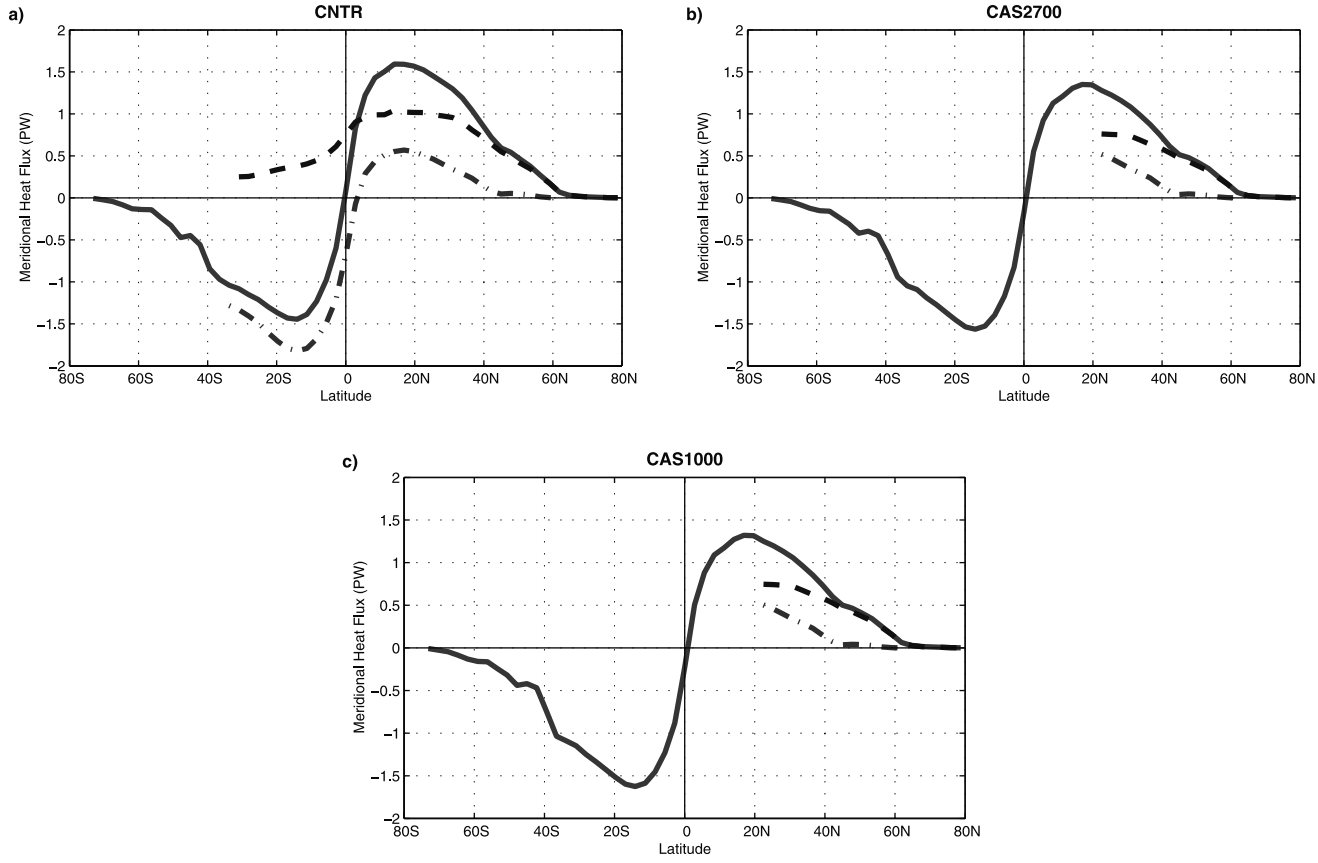

Figure 6. Total PHT in units of PW, where 10^{15} W = 1 PW for the Global (solid red line), Atlantic (dashed blue line), and Indo-Pacific (dash-dotted green line) basins. Positive and negative values imply northward and southward transport, respectively.

change is significantly smaller than that found by *Maier-Reimer et al.* [1990]. One reason for this is that the low surface salinity in the subpolar North Atlantic of the Hamburg model is not caused solely by the influx of Pacific water, which has a mean salinity about 1.5 psu lower than the Atlantic [*Broecker*, 1989]. The salinity is also reduced by the import of Arctic water, as the northeastward flow in the subpolar North Atlantic switches to southwestward. This effect is not observed in the experiments with the MIT OGCM, as the model does not include a representation of the Arctic Ocean. At the same time, the northward flowing Gulf Stream and North Atlantic Drift remain relatively strong when the CAS is open, preventing the southward flow of fresher water from the northernmost part of the basin.

[27] Earlier model studies, including studies with the Hamburg OGCM, suggest that more than one mode of meridional overturning circulation may exist in experiments with modern bathymetry and identical boundary conditions [e.g., *Broecker et al.*, 1985; *Manabe and Stouffer*, 1988; *Marotzke and Willebrand*, 1991; *Maier-Reimer et al.*, 1993]. To test whether the MIT OGCM can exhibit additional steady states, experiment CAS2700 is initialized with fields of homogeneous salinity and stratified, horizontally uniform temperature, instead of the full temperature and salinity fields of *Levitus and Boyer* [1994] and *Levitus et al.* [1994]. Except for these fields, all the boundary conditions remain the same. When integrated the model converges toward the same equilibrium state as the original experiment. Thus, the model gives the same solution with different initial conditions, and there are no indications of secondary modes of circulation.

[28] The test described above is not sufficient to rule out the possible existence of multiple steady states. However, during the course of this study, as well as numerous other experiments with the MIT OGCM, there is no evidence of multiple steady states of the ocean circulation. It is conceivable that the lack of a full Arctic basin in the present model configuration reduces the magnitude of the freshening in the North Atlantic as well as the change in deep water formation in response to an open CAS. However, it is unlikely that the circulation would switch to a steady state without NADW formation.

[29] The increased stability of the meridional overturning circulation in the MIT OGCM is believed to be mainly due to improvements in the surface boundary conditions and the parameterization of mixing due to subgrid-scale eddies. In the experiments with the Hamburg model, traditional mixed boundary conditions are used, where the freshwater flux is diagnosed from a control run with restoring of the surface fields to observed temperatures and salinities. The resulting freshwater flux does not agree well

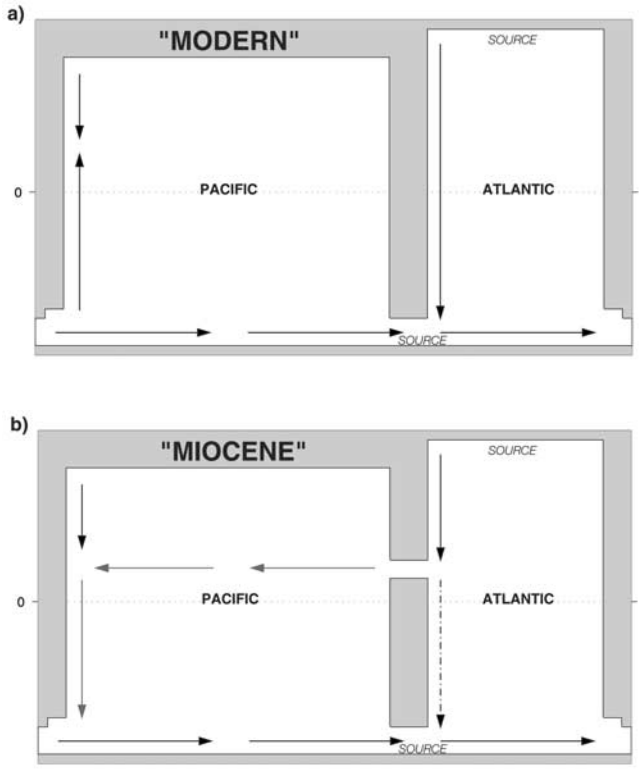

Figure 7. A simplified sketch of the reorganization of the abyssal circulation implied by the model experiments. The interior flow has not been drawn and the only sources of deep water are in the North Atlantic and Southern Ocean. (a) Control experiment with "modern" bathymetry. (b) Perturbed experiment with a CAS extending to depths below the core of NADW.

with observations, and leads to a meridional overturning circulation which is unrealistically sensitive to perturbations in surface salinity [e.g., *Marotzke and Willebrand*, 1991; *Mikolajewicz and Maier-Reimer*, 1994; *Tziperman et al.*, 1994].

4.2. Implications for Neogene Ocean Circulation and Climate

[30] The experiments described in this study employ modern continental configurations and atmospheric forcing. These conditions do not realistically represent the climate of the Miocene and Pliocene, and the results do not represent a simulation of ocean circulation during these periods. Instead, the results test the sensitivity of ocean circulation to a CAS with different depths. The model makes several physically based predictions which might lead to a better understanding of the role of the CAS in ocean circulation and climate. The following predictions can be compared with geochemical and sedimentological tracers from ocean sediment cores: (1) NADW was formed before the final closure of the CAS, (2) a sill depth greater than about 1000 m allows for the passage of a westward jet of NADW into the Pacific Ocean, thus greatly reducing the amount of NADW transported to the South Atlantic, (3) in the western Pacific relatively young NADW flows south as a deep western boundary current, and (4) a shallow sill prevents the flow of NADW to the Pacific and enhances the flow of NADW to the South Atlantic.

4.2.1. Miocene Deep Water Circulation

[31] Data from deep sea sediment cores strongly suggests that NADW was being formed during parts of the middle Miocene (~17–11 Ma) [*Keller and Barron*, 1983; *Miller and Fairbanks*, 1985; *Woodruff and Savin*, 1989], and that the flux of NADW increased in the late Miocene (~11–5 Ma) [*Keller and Barron*, 1983; *Woodruff and Savin*, 1989; *Delaney*, 1990; *King et al.*, 1997], approaching modern values at the time of the final closure of the CAS in the early Pliocene (~5–3 Ma) [*Tiedemann and Franz*, 1997; *Haug and Tiedemann*, 1998; *Billups et al.*, 1999]. While these observations are consistent with this study, the model results also demonstrate that as the CAS shoaled it could have caused dramatic changes to the intermediate and deep circulation in the tropical Pacific, and along the western boundaries of the South Pacific and South Atlantic. It should be possible to test these findings with tracer data from deep sediment cores in these regions.

[32] A common procedure used to infer the relative influences of NADW and AABW in the Atlantic basin has been to compare paleo tracer data (such as $\delta^{13}C$ and *Cd*/*Ca*) from core sites in the Atlantic and Pacific. Convergence of tracer data between the two basins has typically been interpreted as evidence of NADW being replaced in the Atlantic basin by water of Southern Ocean (Pacific) origin [e.g., *Delaney*, 1990; *Wright et al.*, 1992]. However, the model experiments presented here (Figure 4b) suggest that cores in the western South Pacific and western Atlantic could have been influenced by a common water mass during the middle Miocene, with age and nutrient characteristics similar to modern NADW. In other words, convergence of geochemical tracers could indicate NADW in both basins, not water of Pacific or Southern Ocean origin.

[33] *Delaney* [1990], in a study of relative cadmium content (*Cd*/*Ca*) of Miocene benthic foraminifera from the deep South Atlantic (Site 289) and deep western equatorial Pacific (Site 525), showed that the difference in *Cd*/*Ca* ratio between the Atlantic and Pacific was negligible in the early Miocene, small in the middle Miocene, and relatively large in the late Miocene. This data can be interpreted to indicate that relatively young NADW from the CAS could have been present in the western equatorial Pacific during the early and middle Miocene. Similarly, a study comparing benthic foraminiferal $\delta^{13}C$ data from cores in the North Atlantic (Deep Sea Drilling Project (DSDP) 563) and western equatorial Pacific (DSDP 289) [*Wright et al.*, 1992], shows a negligible difference between North Atlantic and South Pacific $\delta^{13}C$ values during the early middle Miocene (15–13 Ma), again consistent with the model predictions.

[34] The sill depth is of great importance in controlling the flow in the CAS. A study of the foraminiferal biostra-

tigraphy of the Atrato Basin in northern South America during the Neogene (~24–2 Ma) [*Duque-Caro*, 1990], indicates that there was a major uplift of the sill to a depth of about 1000 m during the middle Miocene, at ~13–12 Ma, disrupting the exchange of deep water between the Atlantic and Pacific Oceans. This would be analogous to a transition from experiments CAS2700 to CAS1000, and would predict that relatively young NADW would no longer be entering the Pacific via the CAS.

[35] The proposed time for the shoaling of the CAS is close in time to observed increases in NADW formation [*Keller and Barron*, 1983; *Woodruff and Savin*, 1989; *Delaney*, 1990; *King et al.*, 1997], as well as the late Miocene "carbonate crash." Studies from Leg 138 of the Ocean Drilling Program (ODP) find that the east equatorial Pacific was characterized by relatively high carbonate concentrations and accumulation rates before about 11 Ma. However, the accumulation rates declined between 11 and 9.8 Ma, and at about 9.5 Ma, an almost complete loss of carbonate was observed [*Lyle et al.*, 1995; *Farrell et al.*, 1995]. According to *Lyle et al.* [1995], the carbonate crash could not have been caused by an abrupt increase in productivity, or by loss of organic carbon from continental shelves. Instead, the authors conclude that the crash was probably caused by a relatively small reduction in deep water exchange between the Atlantic and Pacific Oceans through the CAS [*Lyle et al.*, 1995; *Farrell et al.*, 1995]. This interpretation is fully consistent with this study, and suggests that the CAS shoaled to less than 1000 m depth by the late Miocene. At this time, the deep water exchange was cut off and in the Pacific carbonate saturated NADW was replaced with older, carbonate undersaturated deep water from the Southern Ocean.

[36] Starting about 10.5 Ma, close in time to the east equatorial carbonate crash, ODP Leg 154 sites at Ceara Rise in the west equatorial Atlantic, experienced a permanent increase in carbonate preservation [*King et al.*, 1997]. Again, this agrees with the model results that predict an increased influence of less corrosive NADW in the South Atlantic as the CAS shoals to 1000 m depth.

4.2.2. Pliocene Climate Change

[37] While the exact sequence of tectonic events leading to the shoaling of the CAS are uncertain [e.g., *Droxler et al.*, 1998; *Mann*, 1999], the timing of the final closure is better constrained. An early study by *Keigwin* [1982], compares $\delta^{18}O$ and $\delta^{13}C$ values of benthic and planktonic foraminifera from DSDP sites in the eastern Pacific and western Caribbean, covering a period ~8–2 Ma. From the $\delta^{18}O$ data it is found that the salinity of Caribbean surface waters started increasing ~4.6 Ma. Further, the $\delta^{13}C$ difference between the two basins increased at ~6 Ma and again at ~3 Ma, approaching modern values. From these data, *Keigwin* [1982] estimated that the final closure of the CAS took place about 3 Ma. Supporting these results are data presented by *Marshall et al.* [1982], which show that the exchange of marine organisms across the CAS was eliminated ~3 Ma, while the exchange of terrestrial biota between the two continents was enhanced.

[38] The proximity of the final closure of the CAS to the onset of enhanced northern hemisphere glaciation ~2.9–2.6 Ma [*Shackleton et al.*, 1984; *Raymo*, 1994; *Maslin et al.*, 1996; *Spielhagen et al.*, 1997] has prompted several authors to connect the two events [*Kaneps*, 1979; *Keigwin*, 1982; *Stanley*, 1995; *Haug and Tiedemann*, 1998; *Driscoll and Haug*, 1998]. According to the study by *Haug and Tiedemann* [1998], the closure of the CAS strengthened the Gulf Stream and the transport of warm saline water to high latitudes of the North Atlantic. This increased the production of NADW, leading to greater evaporative cooling of surface waters and increased atmospheric moisture content. Combined with favorable orbital obliquity, the enhanced moisture content facilitated a buildup of ice sheets in the Northern Hemisphere. The study by *Driscoll and Haug* [1998] proposes a similar mechanism, involving enhanced freshwater delivery to the Arctic via Siberian rivers and the formation of sea ice.

[39] The differences between experiments CAS1000 and CNTR imply that the production of NADW increased at the time of the final closure of the CAS, in agreement with the studies of *Haug and Tiedemann* [1998] and *Driscoll and Haug* [1998]. However, the increased strength of the meridional overturning circulation also implies that additional heat is transported to high latitudes of the North Atlantic (Figure 6). According to the model experiments, the total global PHT is enhanced by about 10% when the CAS is closed, due mostly to a 30% increase in the PHT by the North Atlantic. Indeed, *Berger and Wefer* [1996] have suggested that such an increase in PHT may have delayed the onset of Northern Hemisphere glaciation by several million years, and may possibly have been the cause of the early Pliocene warm period (~5–3) [e.g., *Dowsett et al.*, 1996; *Crowley*, 1996]. Both interpretations above are consistent with the model results: It is not clear whether the effect of the heat or the moisture fluxes dominates in controlling the growth of Northern Hemisphere ice sheets. To further investigate the effect of the final closure of the CAS on the onset of Northern Hemisphere glaciation, it will be necessary to include an atmospheric component to the ocean model. With such a coupled ocean–atmosphere model it will be possible to model changes to the heat and moisture transport by the atmosphere induced by the closure of the CAS.

5. Summary and Conclusions

[40] Experiments with the MIT OGCM were performed to investigate the response of ocean circulation to the shoaling and eventual closure of the CAS. Three model experiment were conducted: A control experiment with modern bathymetry, and two experiments with a CAS with sill depths of 2700 and 1000 m. The model experiments make several physically based predictions, providing a new framework with which to interpret Miocene geochemical tracer data:

1. Deep water is formed in the North Atlantic when the CAS is open, in agreement with Miocene and Pliocene geochemical tracer data. However, the formation rate is reduced by about 10% compared to the control experiment.

2. The reduced rate of NADW formation is due to a flow of relatively fresh water from the Pacific to the Atlantic in the

upper 1000 m of the CAS. The flow increases in strength below the surface to a maximum at a depth of about 500 m.

3. A sill depth greater than about 1000 m allows for the passage of a westward jet of NADW into the Pacific Ocean, thus greatly reducing the amount of NADW transported to the South Atlantic.

4. In the western Pacific, the NADW flows southward as a deep western boundary current, eventually joining the ACC. The presence of relatively young NADW in the western Pacific is consistent with records of $\delta^{13}C$ and *Cd*/*Ca*, which show similar values in the western Pacific and western Atlantic during the middle Miocene.

5. In response to the reduced export of NADW to the South Atlantic, the amount of imported South Atlantic surface water is reduced. The result is a warming of surface waters in the South Atlantic, and an increase in southward heat transport.

6. As the CAS shoals, the flow of NADW to the Pacific is prevented, and the flow of NADW to the South Atlantic is enhanced, creating the modern deep water circulation pattern. This change in the path of relatively young carbonate saturated NADW, is consistent with sediment core data. The data show a loss of carbonate in the east equatorial Pacific and an increase in carbonate preservation in the west equatorial Atlantic at the middle to late Miocene boundary, when the CAS is believed to have shoaled to intermediate depths.

[41] **Acknowledgments.** We are grateful to Veronique Bugnion, Baylor Fox-Kemper, Jeff Scott, John Marshall, Jochem Marotzke, and Ed Boyle for their encouragement and helpful comments. We would also like to thank Tom Crowley and Uwe Mikolajewicz for their valuable comments on an earlier version of this paper. Funding for M.E.R. was provided by MGG NSF grant OCE-0049011.

References

Baumgartner, A., and E. Reichel, *The World Water Balance*, 179 pp., Elsevier Sci., New York, 1975.

Berger, H. W., and G. Wefer, Expedition into the past: Paleoceanographic studies in the South Atlantic, in *The South Atlantic: Present and Past Circulation*, edited by G. Wefer et al., pp. 363–410, Springer-Verlag, New York, 1996.

Bifflups, K., A. C. Ravelo, J. C. Zachos, and R. D. Norris, Link between oceanic heat transport, thermohaline circulation, and the Intertropical Convergence Zone in the early Pliocene Atlantic, *Geology*, *27*(4), 319–322, 1999.

Broecker, W. S., The salinity contrast between the Atlantic and Pacific Oceans during glacial time, *Paleoceanography*, *4*, 207–212, 1989.

Broecker, W. S., D. M. Peteet, and D. Rind, Does the ocean–atmosphere system have more than one stable mode of operation, *Nature*, *315*, 21–26, 1985.

Bryan, K., Accelerating the convergence to equilibrium of ocean climate models, *J. Phys. Oceanogr.*, *14*, 666–673, 1984.

Coates, A. G., J .B. C. Jackson, J. S. Collins, T. M. Cronin, H. J. Dowsett, L. M. Bybell, P. Jung, and J. A. Obando, Closure of the Isthmus of Panama: The near-shore marine record of Costa Rica and western Panama, *Geol. Soc. Am. Bull.*, *104*, 814–828, 1992.

Crowley, T. J., Pliocene climates: The nature of the problem, *Mar. Micropaleontol.*, *27*, 3–12, 1996.

Danabasoglu, G., J. C. McWilliams, and W. G. Large, Approach to equilibrium in accelerated global oceanic models, *J. Clim.*, *9*, 1092–1110, 1996.

Delaney, L. M., Miocene benthic foraminiferal Cd/Ca records: South Atlantic and western equatorial Pacific, *Paleoceanography*, *5*, 743–760, 1990.

Dowsett, H., J. Barron, and R. Poore, Middle Pliocene sea surface temperatures: A global reconstruction, *Mar. Micropaleontol.*, *27*, 13–25, 1996.

Driscoll, N. W., and G. H. Haug, A short circuit in thermohaline circulation: A cause for Northern Hemisphere glaciation?, *Science*, *282*, 436–438, 1998.

Droxler, A. W., K. C. Burke, A. D. Cunningham, A. C. Hine, E. Rosencrantz, D. S. Duncan, P. Hallock, and E. Robinson, Caribbean constraints on circulation between Atlantic and Pacific oceans over the past 40 million years, in *Tectonic Boundary Conditions for Climate Reconstructions*, edited by T. J. Crowley and K. C. Burke, pp. 169–191, Oxford Univ. Press, New York, 1998.

Duque-Caro, H., Neogene stratigraphy, paleoceanography and paleobiogeography in northwest South America and the evolution of the Panama Seaway, *Palaeogeogr. Palaeoclimatol. Palaeoecol.*, *77*, 203–234, 1990.

Farrell, J. W., I. Raffi, T. R. Janacek, D. W. Murray, M. Levitan, K. A. Dadey, K.-C. Emeis, M. Lyle, J.-A. Flores, and S. Hovan, Late Neogene sedimentation patterns in the eastern equatorial Pacific Ocean, in *Proc. Ocean Drill. Program Sci. Results*, vol. 138, edited by N. G. Pisias et al., pp. 717–756, Ocean Drill. Program, College Station, Tex., 1995.

Ganachaud, A. S., Large scale oceanic circulation and fluxes of freshwater, heat, nutrients and oxygen, doctoral dissertation thesis, Mass. Inst. of Technol., Cambridge, Mass., 1999.

Ganachaud, A. S., and C. Wunsch, Improved estimates of global ocean circulation, heat transport and mixing from hydrographic data, *Nature*, *408*, 453–456, 2000.

Gent, P. R., and J. C. McWilliams, Isopycnal mixing in ocean circulation models, *J. Phys. Oceanogr.*, *20*, 150–155, 1990.

Griffies, S. M., The Gent–McWilliams skew flux, *J. Phys. Oceanogr.*, *28*, 831–841, 1998.

Haug, G. H., and R. Tiedemann, Effect of the formation of the Isthmus of Panama on Atlantic Ocean thermohaline circulation, *Nature*, *393*, 673–676, 1998.

Jiang, S., P. H. Stone, and P. Malanotte-Rizzoli, An assessment of the Geophysical Fluid Dynamics Laboratory ocean model with coarse resolution: Annual-mean climatology, *J. Geophys. Res.*, *104*(C11), 25,623–25,645, 1999.

Kamenkovich, I. V., A. Sokolov, and P. H. Stone, An efficient climate model with a 30 ocean and statistical-dynamical atmosphere, *Clim. Dyn.*, *19*, 585–598, 2002.

Kaneps, A. G., Gulf Stream: Velocity fluctuations during the late Cenozoic, *Science*, *204*, 297–301, 1979.

Keigwin, L., Isotopic paleoceanography of the Caribbean and East Pacific: Role of Panama uplift in Late Neogene time, *Science*, *217*, 350–352, 1982.

Keller, G., and J. A. Barron, Paleoceanographic implications of the Miocene deep-sea hiatuses, *Geol. Soc. Am. Bull.*, *94*, 590–613, 1983.

King, T. A., W. G. Ellis Jr., D. W. Murray, N. J. Shackleton, and S. Harris, Miocene evolution of carbonate sedimentation at the Ceara rise: A multivariate data/proxy approach, in *Proc. Ocean Drill. Program Sci. Results*, edited by N. J. Shackleton et al., pp. 349–365, Ocean Drill. Program, College Station, Tex., 1997.

Levitus, S., and T. P. Boyer, *World Ocean Atlas 1994 Volume 4: Temperature*, 117 pp., U.S. Dept. of Commer., Washington, D. C., 1994.

Levitus, S., R. Burgett, and T. P. Boyer, *World Ocean Atlas 1994 Volume 3: Salinity*, 99 pp., U.S. Dept. of Commer., Washington, D. C., 1994.

Lyle, M., K. A. Dadey, and J. W. Farrell, The Late Miocene (11–8 Ma) eastern Pacific carbonate crash: Evidence for reorganization of deep-water circulation by the closure of the Panama gateway, in *Proc. Ocean Drill. Program Sci. Results*, edited by N. G. Pisias et al., pp. 821–838, Ocean Drill. Program, College Station, Tex., 1995.

Maier-Reimer, E., U. Mikolajewicz, and T. Crowley, Ocean general circulation model sensitivity experiment with an open Central American isthmus, *Paleoceanography*, *5*, 349–366, 1990.

Maier-Reimer, E., U. Mikolajewicz, and K. Hasselmann, Mean circulation of the Hamburg LSG OGCM and its sensitivity to the thermohaline surface forcing, *J. Phys. Oceanogr.*, *23*, 731–757, 1993.

Manabe, S., and R. J. Stouffer, Two stable equilibria of a coupled ocean–atmosphere model, *J. Clim.*, *1*, 841–866, 1988.

Mann, P., Caribbean sedimentary basins: Classification and tectonic setting from Jurassic to present, in *Caribbean Basins*, edited by P. Mann, pp. 3–31, Elsevier Sci., New York, 1999.

Marotzke, J., and J. Willebrand, Multiple equilibria of the global thermohaline circulation, *J. Phys. Oceanogr.*, *21*, 1372–1385, 1991.

Marshall, J., and F. Schott, Open-ocean convection: Observations, theory, and models, *Rev. Geophys.*, *37*(1), 1–64, 1999.

Marshall, J., A. Adcroft, C. Hill, L. Perelman, and C. Heisey, A finite-volume, incompressible Navier Stokes model for studies of the ocean on parallel computers, *J. Geophys. Res.*, *102*(C3), 5753–5766, 1997a.

Marshall, J., C. Hill, L. Perelman, and A. Adcroft, Hydrostatic, quasi-hydrostatic, and nonhydrostatic ocean modeling, *J. Geophys. Res.*, *102*(C3), 5733–5752, 1997b.

Marshall, L. G., S. D. Webb, J. J. Sepkoski, and D. M. Raup, Mammalian evolution and the great American interchange, *Science*, *215*, 1351–1357, 1982.

Maslin, M. A., G. H. Haug, M. Sarntheim, and R. Tiedemann, The progressive intensification of Northern Hemisphere glaciation as seen from the North Pacific, *Geol. Rundsch.*, *85*, 452–465, 1996.

Mikolajewicz, U., and T. J. Crowley, Response of a coupled ocean/energy balance model to restricted flow through the central American isthmus, *Paleoceanography*, *12*, 429–441, 1997.

Mikolajewicz, U., and E. Maier-Reimer, Mixed boundary-conditions in ocean general-circulation models and their influence on the stability of the models conveyor belt, *J. Geophys. Res.*, *99*(C11), 22,633–22,644, 1994.

Mikolajewicz, U., E. Maier-Reimer, T. J. Crowley, and K. Y. Kim, Effect of Drake and Panamanian Gateways on the circulation of an ocean model, *Paleoceanography*, *8*, 409–426, 1993.

Miller, K. G., and R. G. Fairbanks, Oligocene to Miocene carbon isotope cycles and abyssal circulation changes, in *The Carbon Cycle and Atmospheric CO2: Natural Variations Archean to Present*, edited by E. T. Sundquist and W. S. Broecker, pp. 469–486, AGU, Washington, D. C., 1985.

Perry, G. D., P. B. Duffy, and N. L. Miller, An extended data set of river discharges for validation of general circulation models, *J. Geophys. Res.*, *101*(D16), 21,339–21,349, 1996.

Raymo, M. E., The initiation of Northern Hemisphere glaciation, *Annu. Rev. Earth Planet. Sci.*, *22*, 353–383, 1994.

Redi, M. H., Oceanic isopycnal mixing by coordinate rotation, *J. Phys. Oceanogr.*, *12*, 1154–1158, 1982.

Reeh, N., Calving from Greenland glaciers: Observations, balance estimates of calving rate, calving laws, in *Workshop on the Calving Rate of West Greenland Glaciers in Response to Climate Change*, p. 171, Dan. Polar Cent., Copenhagen, 1994.

Schmitt, R. W., P. S. Bogden, and C. E. Dorman, Evaporation minus precipitation and density fluxes for the North Atlantic, *J. Phys. Oceanogr.*, *19*, 1208–1221, 1989.

Shackleton, N. J., et al., Oxygen isotope calibration of the onset of ice-rafting and history of glaciation in the North Atlantic region, *Nature*, *307*, 620–623, 1984.

Spielhagen, R. F., et al., Arctic ocean evidence for late Quaternary initiation of northern Eurasian ice sheets, *Geology*, *25*(9), 783–786, 1997.

Stanley, S. M., New horizons for paleontology with two examples: The rise and fall of the Cretaceous supertethys and the cause of the modern ice age, *J. Paleontol.*, *69*(6), 999–1007, 1995.

Stommel, H., and A. B. Arons, On the abyssal circulation of the world ocean, 1, Stationary planetary flow patterns on a sphere, *Deep Sea Res.*, *6*, 140–154, 1960a.

Stommel, H., and A. B. Arons, On the abyssal circulation of the world ocean, 2, An idealized model of the circulation pattern and amplitude in oceanic basins, *Deep Sea Res.*, *6*, 217–233, 1960b.

Tiedemann, R., and S. O. Franz, Deep-water circulation, chemistry, and terrigenous sediment supply in the equatorial Atlantic during the Pliocene, 3.3–2.6 Ma and 5–4.5 Ma, in *Proc. Ocean Drill. Program Sci. Results*, edited by N. J. Shackleton et al., pp. 299–318, Ocean Drill. Program, College Station, Tex., 1997.

Trenberth, K. E., and A. Solomon, The global heat-balance: Heat transports in the atmosphere and ocean, *Clim. Dyn.*, *10*(3), 107–134, 1994.

Trenberth, K. E., J. G. Olson, and W. G. Large, A global ocean wind stress climatology based on ECMWF analysis, *NCAR Tech. Note*, NCAR/TN-338+STR, Natl. Cent. for Atmos. Res., Boulder, Colo., 1989.

Tziperman, E., J. R. Toggweiler, Y. Feliks, and K. Bryan, Instability of the thermohaline circulation with respect to mixed boundary-conditions: Is it really a problem for realistic models, *J. Phys. Oceanogr.*, *24*, 217–232, 1994.

Woodruff, F., and S. Savin, Miocene deep-water oceanography, *Paleoceanography*, *4*, 87–140, 1989.

Wright, J. D., K. G. Miller, and R. G. Fairbanks, Early and middle Miocene stable isotopes: Implications for deepwater circulation and climate, *Paleoceanography*, *7*, 357–389, 1992.

K. H. Nisancioglu and P. H. Stone, Program in Atmosphere, Oceans, and Climate, Department of Earth, Atmospheric, and Planetary Sciences, Massachusetts Institute of Technology, Cambridge, MA 02141, USA. (kerim@mit.edu; phstone@mit.edu)

M. E. Raymo, Department of Earth Sciences, Boston University, 685 Commonwealth Avenue, Boston, MA 02215, USA. (raymo@bu.edu)